

DSelect-k: Differentiable Selection in the Mixture of Experts with Applications to Multi-Task Learning

Hussein Hazimeh¹, Zhe Zhao², Aakanksha Chowdhery², Maheswaran Sathiamoorthy²
Yihua Chen², Rahul Mazumder¹, Lichan Hong², Ed H. Chi²

¹Massachusetts Institute of Technology, {hazimeh, rahulmaz}@mit.edu

²Google Brain, {zhezha, chowdhery, nlogn, yhchen, lichan, edchi}@google.com

Abstract

The Mixture-of-experts (MoE) architecture is showing promising results in multi-task learning (MTL) and in scaling high-capacity neural networks. State-of-the-art MoE models use a trainable “sparse gate” to select a subset of the experts for each input example. While conceptually appealing, existing sparse gates, such as Top-k, are not smooth. The lack of smoothness can lead to convergence and statistical performance issues when training with gradient-based methods. In this paper, we develop DSelect-k: the first, continuously differentiable and sparse gate for MoE, based on a novel binary encoding formulation. Our gate can be trained using first-order methods, such as stochastic gradient descent, and offers explicit control over the number of experts to select. We demonstrate the effectiveness of DSelect-k in the context of MTL, on both synthetic and real datasets with up to 128 tasks. Our experiments indicate that MoE models based on DSelect-k can achieve statistically significant improvements in predictive and expert selection performance. Notably, on a real-world large-scale recommender system, DSelect-k achieves over 22% average improvement in predictive performance compared to the Top-k gate. We provide an open-source TensorFlow implementation of our gate¹.

1 Introduction

The Mixture of Experts (MoE) [14] is the basis of many state-of-the-art deep learning models. For example, MoE-based layers are being used to perform efficient computation in high-capacity neural networks and to improve parameter sharing in multi-task learning (MTL) [33, 22, 21]. While different MoE architectures are considered in the literature, two major components are needed in any MoE model: a set of experts (neural networks) and one or more trainable gates. A gate selects a combination of the experts that is specific to each input example. This allows experts to specialize in different partitions of the input space, which has the potential to improve the predictive performance and interpretability. In Figure 1(a), we show an example of a simple MoE architecture that can be used as a standalone learner or as a layer in a neural network.

The literature on the MoE has traditionally focused on softmax-based gates, in which all experts are assigned nonzero weights [17]. More recent works propose *sparse gates* that assign nonzero weights to only a small subset of the experts [1, 33, 29, 21]. Sparsity in gating can have various advantages, including better computational efficiency, interpretability, and improved statistical performance in certain settings. Existing sparse gates are not differentiable, and reinforcement learning algorithms are commonly used to train these gates [1, 29]. In an exciting work, Shazeer et al. [33] introduced a

¹https://github.com/google-research/dselect_k_moe

new sparse gate (Top-k gate) and proposed training it using stochastic gradient descent (SGD). The ability to train the gate using SGD is appealing because it allows for training the neural network in an end-to-end fashion. However, the Top-k gate is not continuous, which can lead to convergence issues in SGD that in turn affect the statistical performance (as we demonstrate in our experiments).

In this paper, we introduce DSelect-k: the first, continuously differentiable and sparse gate for MoE. Given a user-specified parameter k , the gate selects at most k out of the n experts. This explicit control over sparsity leads to a cardinality-constrained optimization problem, which is computationally challenging. To circumvent this challenge, we propose a novel, unconstrained reformulation that is equivalent to the original problem. The reformulated problem uses a binary encoding scheme to implicitly enforce the cardinality constraint. We demonstrate that by carefully smoothing the binary encoding variables, the reformulated problem can be effectively optimized using first-order methods such as SGD.

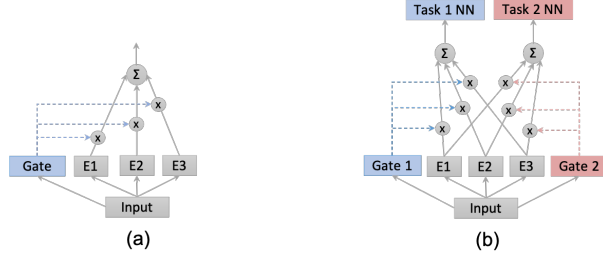


Figure 1: **(a):** An example of a MoE that can be used as a standalone learner or layer in a neural network. “E i ” is the i -th expert. **(b):** A multi-gate MoE for learning two tasks simultaneously. “Task i NN” is a neural network which generates the output of Task i .

Our gate supports two mechanisms: *per-example gating* and *static gating*. The per-example gating is the typical gating technique used in MoE models, in which the weights assigned to the experts are a function of the input example [14, 33]. In static gating, a subset of experts is selected and the corresponding weights do not depend on the input [29]. Based on our experiments, each gating mechanism can outperform the other in certain settings. Thus, we study both mechanisms and advocate for experimenting with each.

MTL is an important area where MoE models in general, and our gate in particular, can be useful. The goal of MTL is to learn multiple tasks simultaneously by using a shared model. Compared to the usual single task learning, MTL can achieve better generalization performance through exploiting the relationships between tasks [4]. One of the key problems in MTL is how to share model parameters between tasks [31]. For instance, sharing parameters between unrelated tasks can potentially degrade performance. The multi-gate MoE [22] is a flexible architecture which allows for learning what to share between tasks. Figure 1(b) shows an example of a multi-gate MoE (in the simple case of two tasks). Here, each task has its own gate which adaptively decides whether to share experts with the other task. In our experiments, we study the effectiveness of our proposed gate in the context of the multi-gate MoE.

Contributions: On a high-level, our main contribution is DSelect-k: a new continuously differentiable and sparse gate for MoE, which can be directly trained using first-order methods. Our technical contributions can be summarized as follows. **(i)** The gate selects (at most) k out of the n experts, where k is a user-specified parameter. This leads to a challenging, cardinality-constrained optimization problem. To deal with this challenge, we develop a novel, unconstrained reformulation and we prove that it is equivalent to the original problem. The reformulation uses a binary encoding scheme that implicitly imposes the cardinality constraint using learnable binary codes. **(ii)** To make the unconstrained reformulation smooth, we relax and smooth the binary variables. We demonstrate that, with careful initialization and regularization, the resulting problem can be optimized with first-order methods such as SGD. **(iii)** We carry out a series of experiments on synthetic and real MTL datasets, which show that our gate outperforms state-of-the-art gates in terms of parameter sharing and predictive performance. **(iv)** We provide an open-source implementation of DSelect-k.

1.1 Related Work

MoE and Conditional Computation: Since MoE was introduced by Jacobs et al. [14], an exciting body of work has extended and studied this model, e.g., see Jordan and Jacobs [17], Jacobs [13], Jiang

and Tanner [16]. Recently, MoE-based models are showing success in deep learning. For example, Shazeer et al. [33] introduced the sparse Top-k gate for MoE and showed significant computational improvements on machine translation tasks; we discuss exact connections to this gate in Section 2. The Top-k gate has also been utilized in several state-of-the-art deep learning models that considered MTL tasks, e.g., Lepikhin et al. [21], Ramachandran and Le [28], Fedus et al. [9]. Our work is also related to the conditional computation models that activate parts of the neural network based on the input [1]. These models use a trainable gate that decides which part of the neural network to activate for each input example, with the goal of speeding up training or inference. Works in this area include [2, 1, 33, 12, 36]. Unlike our work, these works are based on non-differentiable models, or heuristics where the training and inference models are different.

Stochastic Subset Selection and Sparse Transformations: A related line of work develops mechanisms for stochastic subset selection in neural networks, e.g., see [26, 5, 39] and the references therein. Specifically, these works allow for sampling k -subsets from a categorical distribution, based on extensions or generalizations of the Gumbel-softmax trick [23, 15]. However, in the MoE we consider *deterministic* subset selection—determinism is a common assumption in MoE models (for example, in [14, 17, 33]) that can improve interpretability. In contrast, the approaches described above assume stochastic selection and are suitable in applications where there is an underlying sampling distribution, such as in variational inference [19]. In Appendix A, we provide more context, and we discuss important differences between our proposal and these approaches. In addition, a related body of work has developed sparse transformations as alternatives to the softmax function, e.g., the sparsemax [24] and its generalizations [27, 6, 3]. However, there is an important distinction: our formulation imposes a cardinality constraint that controls the number of nonzeros precisely, whereas the latter approaches do not impose a cardinality constraint (e.g., sparsemax cannot control sparsity). The cardinality constraint is important for interpretability and computational efficiency in MoE because all examples or tasks will respect the desired sparsity level (in contrast, sparse transformations that do not precisely control sparsity, may assign some examples or tasks sparse combinations and others dense combinations).

MTL: In Appendix A, we review related literature on MTL.

2 Gating in the Mixture of Experts

In this section, we first review the MoE architecture and popular gates, and then discuss how these gates compare to our proposal. We will assume that the inputs to the MoE belong to a space $\mathcal{X} \subset \mathbb{R}^p$. In its simplest form, the MoE consists of a set of n experts (neural networks) $f_i : \mathcal{X} \rightarrow \mathbb{R}^u$, $i \in \{1, 2, \dots, n\}$, and a gate $g : \mathcal{X} \rightarrow \mathbb{R}^n$ that assigns weights to the experts. The gate’s output is assumed to be a probability vector, i.e., $g(x) \geq 0$ and $\sum_{i=1}^n g(x)_i = 1$, for any $x \in \mathcal{X}$. Given an example $x \in \mathcal{X}$, the corresponding output of the MoE is a weighted combination of the experts:

$$\sum_{i=1}^n f_i(x)g(x)_i. \quad (1)$$

Next, we discuss two popular choices for the gate $g(\cdot)$ that can be directly optimized using SGD.

Softmax Gate: A classical model for $g(x)$ is the softmax gate: $\sigma(Ax + b)$, where $\sigma(\cdot)$ is the softmax function, $A \in \mathbb{R}^{n \times p}$ is a trainable weight matrix, and $b \in \mathbb{R}^n$ is a bias vector [17]. This gate is dense, in the sense that all experts are assigned nonzero probabilities. Note that static gating (i.e., gating which does not depend on the input example) can be obtained by setting $A = 0$.

Top-k Gate: This is a sparse variant of the softmax gate that returns a probability vector with only k nonzero entries [33]. The Top-k gate is defined by $\sigma(\text{KeepTopK}(Ax + b))$, where for any vector v , $\text{KeepTopK}(v)_i := v_i$ if v_i is in the top k elements of v , and $\text{KeepTopK}(v)_i := -\infty$ otherwise². This gate is conceptually appealing since it allows for direct control over the number of experts to select and is trained using SGD. Moreover, the Top-k gate supports *conditional training*: in backpropagation, for each input example, only the gradients of the loss w.r.t. top k elements need to be computed. With a careful implementation, conditional training can lead to computational savings. However, the Top-k gate is not continuous, which implies that the gradient does not exist at certain inputs. This

²To help in load balancing across the experts, Shazeer et al. [33] add Gaussian noise and additional regularizers to the model.

can be problematic when training is done using gradient-based methods. To gain more insight, in Appendix C.3, we plot the expert weights chosen by the Top-k gate during training with SGD. The results indicate an oscillatory behavior in the output of the Top-k gate, which can be attributed to its discontinuous nature: a small change in the input can lead to “jumps” in the output.

Comparison with DSelect-k: We develop DSelect-k in Section 3. Here we present a high-level comparison between DSelect-k and Top-k. Similar to Top-k, DSelect-k can select k out of the n experts and can be trained using gradient-based optimization methods. A major advantage of DSelect-k over Top-k is that it is continuously differentiable, which leads to more stable selection of experts during training—see Appendix C.3 for visualizations of the expert weights during training. During inference, DSelect-k only needs to evaluate a subset of the experts, which can lead to computational savings. However, DSelect-k supports conditional training only partially. At the start of training, it uses all the available experts, so conditional training is not possible. As we discuss in Section 3, after a certain point during training, DSelect-k converges to a small subset of the experts, and then conditional training becomes possible. Our experiments indicate that DSelect-k has a significant edge over Top-k in terms of prediction and expert selection performance, so the full support for conditional training in Top-k comes at the expense of statistical performance.

3 Differentiable and Sparse Gating

In this section, we develop the DSelect-k gate, for both the static and per-example gating settings. First, we introduce the problem setup and notation. To simplify the presentation, we will develop the gate for a single supervised learning task, and we note that the same gate can be used in MTL models. We assume that the task has an input space $\mathcal{X} \subset \mathbb{R}^p$, an output space \mathcal{Y} , and an associated loss function $\ell : \mathcal{Y} \times \mathbb{R} \rightarrow \mathbb{R}$. We denote the set of N training examples by $\mathcal{D} = \{(x_i, y_i) \in \mathcal{X} \times \mathcal{Y}\}_{i=1}^N$. We consider a learning model defined by the MoE in Equation (1). For simplicity, we assume that the experts are scalar-valued and belong to a class of continuous functions \mathcal{H} . We assume that the number of experts $n = 2^m$ for some integer m —in Appendix B.2, we discuss how the gate can be extended to arbitrary n . For convenience, given a non-negative integer i , we denote the set $\{1, 2, \dots, i\}$ by $[i]$.

In Section 3.1, we develop DSelect-k for the static gating setting. Then, in Section 3.2, we generalize it to the per-example setting.

3.1 DSelect-k for Static Gating

Our goal here is to develop a static gate that selects a convex combination of at most k out of the n experts. The output of the gate can be thought of as a probability vector w with at most k nonzero entries, where w_i is the weight assigned to the expert f_i . A natural way to minimize the empirical risk of the MoE model is by solving the following problem:

$$\min_{f_1, \dots, f_n, w} \quad \frac{1}{N} \sum_{(x, y) \in \mathcal{D}} \ell\left(y, \sum_{i=1}^n f_i(x) w_i\right) \quad (2a)$$

$$\text{s.t.} \quad \|w\|_0 \leq k \quad (2b)$$

$$\sum_{i=1}^n w_i = 1, \quad w \geq 0. \quad (2c)$$

In the above, the L_0 norm of w , $\|w\|_0$, is equal to the number of nonzero entries in w . Thus, the cardinality constraint (2b) ensures that the gate selects at most k experts. Problem (2) is a combinatorial optimization problem that is not amenable to SGD due to the cardinality constraint (2b) and the simplex constraints in (2c). In what follows of this section, we first transform Problem (2) into an equivalent unconstrained optimization problem, based on a binary encoding scheme. However, the unconstrained problem cannot be directly handled using SGD due to the presence of binary variables. Thus, in a second transformation, we smooth the binary variables, which leads to an optimization problem that is amenable to SGD.

Roadmap: In Section 3.1.1, we introduce the *single expert selector*: a construct for choosing 1 out of n experts by using binary encoding. In Section 3.1.2, we leverage the single expert selector to transform Problem (2) into an unconstrained one. Then, in Section 3.1.3, we smooth the unconstrained problem and discuss how SGD can be applied.

3.1.1 Single Expert Selection: Binary Encoding

The single expert selector (selector, for short) is a fundamental construct that we will later use to convert Problem (2) to an unconstrained optimization problem. At a high-level, the single expert selector chooses the index of 1 out of the n experts and returns a one-hot encoding of the choice. For example, in the case of 4 experts, the selector can choose the first expert by returning the binary vector $[1\ 0\ 0\ 0]^T$. Generally, the selector can choose any of the experts, and its choice is determined by a set of binary encoding variables, as we will describe next.

The selector is parameterized by m (recall that $m = \log_2 n$) binary variables, z_1, z_2, \dots, z_m , where we view these variables collectively as a binary number: $z_m z_{m-1} \dots z_1$. The integer represented by the latter binary number determines which expert to select. More formally, let l be the integer represented by the binary number $z_m z_{m-1} \dots z_1$. The selector is a function $r : \mathbb{R}^m \rightarrow \{0, 1\}^n$ which maps $z := [z_1, z_2, \dots, z_m]^T$ to a one-hot encoding of the integer $(l + 1)$. For example, if all the z_i 's are 0, then the selector returns a one-hot encoding of the integer 1. Next, we define the selector $r(z)$. For easier exposition, we start with the special case of 4 experts and then generalize to n experts.

Special case of 4 experts: In this case, the selector uses two binary variables z_1 and z_2 . Let l be the integer represented by the binary number $z_2 z_1$. Then, the selector should return a one-hot encoding of the integer $(l + 1)$. To achieve this, we define the selector $r(z)$ as follows:

$$r(z) = [\bar{z}_1 \bar{z}_2, \bar{z}_1 z_2, z_1 \bar{z}_2, z_1 z_2]^T \quad (3)$$

where $\bar{z}_i := 1 - z_i$. By construction, exactly one entry in $r(z)$ is 1 (specifically, $r(z)_{l+1} = 1$) and the rest of the entries are zero. For example, if $z_1 = z_2 = 0$, then $r(z)_1 = 1$ and $r(z)_i = 0$ for $i \in \{2, 3, 4\}$.

General case of n experts: Here we generalize the selector $r(z)$ to the case of n experts. To aid in the presentation, we make the following definition. For any non-negative integer l , we define $\mathcal{B}(l)$ as the set of indices of the nonzero entries in the binary representation of l (where we assume that the least significant bit is indexed by 1). For example, $\mathcal{B}(0) = \emptyset$, $\mathcal{B}(1) = \{1\}$, $\mathcal{B}(2) = \{2\}$, and $\mathcal{B}(3) = \{1, 2\}$. For every $i \in [n]$, we define the i -th entry of $r(z)$ as follows:

$$r(z)_i = \prod_{j \in \mathcal{B}(i-1)} (z_j) \prod_{j \in [m] \setminus \mathcal{B}(i-1)} (1 - z_j) \quad (4)$$

In the above, $r(z)_i$ is a product of m binary variables, which is equal to 1 iff the integer $(i - 1)$ is represented by the binary number $z_m z_{m-1} \dots z_1$. Therefore, $r(z)$ returns a one-hot encoding of the index of the selected expert. Note that when $n = 4$, definitions (3) and (4) are equivalent.

3.1.2 Unconstrained Minimization

In this section, we develop a combinatorial gate which allows for transforming Problem (2) into a unconstrained optimization problem. We design this gate by creating k instances of the single expert selector $r(\cdot)$, and then taking a convex combination of these k instances. More formally, for every $i \in [k]$, let $z^{(i)} \in \{0, 1\}^m$ be a (learnable) binary vector, so that the output of the i -th instance of the selector is $r(z^{(i)})$. Let Z be a $k \times m$ matrix whose i -th row is $z^{(i)}$. Moreover, let $\alpha \in \mathbb{R}^k$ be a vector of learnable parameters. We define the *combinatorial gate* q as follows:

$$q(\alpha, Z) = \sum_{i=1}^k \sigma(\alpha)_i r(z^{(i)}),$$

where we recall that $\sigma(\cdot)$ is the softmax function. Since for every $i \in [k]$, $r(z^{(i)})$ is a one-hot vector, we have $\|q(\alpha, Z)\|_0 \leq k$. Moreover, since the weights of the selectors are obtained using a softmax, we have $q(\alpha, Z) \geq 0$ and $\sum_{i=1}^n q(\alpha, Z)_i = 1$. Thus, $q(\alpha, Z)$ has the same interpretation of w in Problem (2), without requiring any constraints. Therefore, we propose replacing w in the objective of Problem (2) with $q(\alpha, Z)$ and removing all the constraints. This replacement leads to an equivalent unconstrained optimization problem, as we state in the next proposition.

Proposition 1. *Problem (2) is equivalent³ to:*

$$\min_{f_1, \dots, f_n, \alpha, Z} \frac{1}{N} \sum_{(x, y) \in \mathcal{D}} \ell\left(y, \sum_{i=1}^n f_i(x) q(\alpha, Z)_i\right) \quad (5)$$

$$z^{(i)} \in \{0, 1\}^m, \quad i \in [k]$$

The proof of Proposition 1 is in Appendix B.1. Unlike Problem (2), Problem (5) does not involve any constraints, aside from requiring binary variables. However, these binary variables cannot be directly handled using first-order methods. Next, we discuss how to smooth the binary variables in order to obtain a continuous relaxation of Problem (5).

3.1.3 Smooth Gating

In this section, we present a procedure to smooth the binary variables in Problem (5) and discuss how the resulting problem can be optimized using first-order methods. The procedure relies on the *smooth-step* function, which we define next.

Smooth-step Function: This is a continuously differentiable and S-shaped function, similar in shape to the logistic function. However, unlike the logistic function, the smooth-step function can output 0 and 1 exactly for sufficiently large magnitudes of the input. The smooth-step and logistic functions are depicted in Appendix B.3. More formally, given a non-negative scaling parameter γ , the smooth-step function, $S : \mathbb{R} \rightarrow \mathbb{R}$, is a cubic piecewise polynomial defined as follows:

$$S(t) = \begin{cases} 0 & \text{if } t \leq -\gamma/2 \\ -\frac{2}{\gamma^3}t^3 + \frac{3}{2\gamma}t + \frac{1}{2} & \text{if } -\gamma/2 \leq t \leq \gamma/2 \\ 1 & \text{if } t \geq \gamma/2 \end{cases}$$

The parameter γ controls the width of the fractional region (i.e., the region where the function is strictly between 0 and 1). Note that $S(t)$ is continuously differentiable at all points—this follows since at the boundary points $\pm\gamma/2$, we have: $S'(-\gamma/2) = S'(\gamma/2) = 0$. This function has been recently used for conditional computation in soft trees [11] and is popular in the literature on computer graphics [8, 30].

Smoothing: We obtain DSelect-k from the combinatorial gate $q(\alpha, Z)$ by (i) relaxing every binary variable in Z to be continuous in the range $(-\infty, +\infty)$, i.e., $Z \in \mathbb{R}^{k \times m}$, and (ii) applying the smooth-step function to Z element-wise. Formally, DSelect-k is a function \tilde{q} defined as follows:

$$\tilde{q}(\alpha, Z) := q(\alpha, S(Z)) = \sum_{i=1}^k \sigma(\alpha)_i r(S(z^{(i)})), \quad (6)$$

where the matrix $S(Z)$ is obtained by applying $S(\cdot)$ to Z element-wise. Note that $\tilde{q}(\alpha, Z)$ is continuously differentiable so it is amenable to first-order methods. If $S(Z)$ is binary, then $\tilde{q}(\alpha, Z)$ selects at most k experts (this holds since $\tilde{q}(\alpha, Z) = q(\alpha, S(Z))$, and from Section 3.1.2, q selects at most k experts when its encoding matrix is binary). However, when $S(Z)$ has any non-binary entries, then more than k experts can be potentially selected, meaning that the cardinality constraint will not be respected. In what follows, we discuss how the gate can be optimized using first-order methods, while ensuring that $S(Z)$ converges to a binary matrix so that the cardinality constraint is enforced.

We propose using $\tilde{q}(\alpha, Z)$ in MoE, which leads to the following optimization problem:

$$\min_{f_1, \dots, f_n, \alpha, Z} \frac{1}{N} \sum_{(x, y) \in \mathcal{D}} \ell\left(y, \sum_{i=1}^n f_i(x) \tilde{q}(\alpha, Z)_i\right) \quad (7)$$

Problem (7) can be viewed as a continuous relaxation of Problem (5). If the experts are differentiable, then the objective of Problem (7) is differentiable. Thus, we propose optimizing MoE end-to-end using first-order methods. We note that $\tilde{q}(\alpha, Z)$ uses $(k + k \log n)$ learnable parameters. In contrast, the Top-k and softmax gates (discussed in Section 2) use n parameters. Thus, for relatively small

³By equivalent we mean that the two problems have the same optimal objective, and given an optimal solution for one problem, we can construct an optimal solution for the other.

k , our proposal uses a smaller number of parameters. Next, we discuss how the DSelect- k gate’s parameters should be initialized in order to ensure that it is trainable.

Initialization: By the definition of the smooth-step function, if $S(Z_{ij})$ is binary then $S'(Z_{ij}) = 0$, and consequently $\frac{\partial \ell}{\partial Z_{ij}} = 0$. This implies that, during optimization, if $S(Z_{ij})$ becomes binary, the variable Z_{ij} will not be updated in any subsequent iteration. Thus, we have to be careful about the initialization of Z . For example, if Z is initialized so that $S(Z)$ is a binary matrix then the gate will not be trained. To ensure that the gate is trainable, we initialize each Z_{ij} so that $0 < S(Z_{ij}) < 1$. This way, the Z_{ij} ’s can have nonzero gradients at the start of optimization.

Accelerating Convergence to Binary Solutions: Recall that we need $S(Z)$ to converge to a binary matrix, in order for the gate \tilde{q} to respect the cardinality constraint (i.e., to select at most k experts). Empirically, we observe that if the optimizer runs for a sufficiently large number of iterations, then $S(Z)$ typically converges to a binary matrix. However, early stopping of the optimizer can be desired in practice for computational and statistical considerations, and this can prevent $S(Z)$ from converging. To encourage faster convergence towards a binary $S(Z)$, we will add an entropy regularizer to Problem (7). The following proposition is needed before we introduce the regularizer.

Proposition 2. *For any $z \in \mathbb{R}^m$, $\alpha \in \mathbb{R}^k$, and $Z \in \mathbb{R}^{k \times m}$, $r(S(z))$ and $\tilde{q}(\alpha, Z)$ belong to the probability simplex.*

The proof of the proposition is in Appendix B.1. Proposition 2 implies that, during training, the output of each single expert selector used by $\tilde{q}(\alpha, Z)$, i.e., $r(S(z^{(i)}))$ for $i \in [k]$, belongs to the probability simplex. Note that the entropy of each $r(S(z^{(i)}))$ is minimized by any one-hot encoded vector. Thus, for each $r(S(z^{(i)}))$, we add an entropy regularization term that encourages convergence towards one-hot encoded vectors; equivalently, this encourages convergence towards a binary $S(Z)$. Specifically, we solve the following regularized variant of Problem (7):

$$\min_{f_1, \dots, f_n, \alpha, Z} \sum_{(x, y) \in \mathcal{D}} \frac{1}{N} \ell\left(y, \sum_{i=1}^n f_i(x) \tilde{q}(\alpha, Z)_i\right) + \lambda \Omega(Z)$$

where $\Omega(Z) := \sum_{i=1}^k h(r(S(z^{(i)})))$ and $h(\cdot)$ is the entropy function. The hyperparameter λ is non-negative and controls how fast each selector converges to a one-hot encoding. In our experiments, we tune over a range of λ values. When selecting the best hyperparameters from tuning, we disregard any λ whose corresponding solution does not have a binary $S(Z)$. In Appendix C.4, we report the number of training steps required for $S(Z)$ to converge to a binary matrix, on several real datasets. Other alternatives to ensure that $S(Z)$ converges to a binary matrix are also possible. One alternative is to regularize the entropy of each entry in $S(Z)$ separately. Another alternative is to anneal the parameter γ of the smooth-step function towards zero.

Softmax-based Alternative to Binary Encoding: Recall that our proposed selectors in (6), i.e., $r(S(z^{(i)}))$, $i \in [k]$, learn one-hot vectors *exactly* (by using binary encoding). One “practical” alternative for learning a one-hot vector is by using a softmax function with temperature annealing (or entropy regularization). Theoretically, this alternative cannot return a one-hot vector, but after training, the softmax output can be transformed to a one-hot vector using a heuristic (e.g., by taking an argmax). In Appendix C.2, we perform an ablation study of our gate in which we replace the selectors with softmax functions (along with temperature annealing or entropy regularization). Although this alternative is heuristic, we consider it due to its popularity.

3.2 DSelect- k for Per-example Gating

In this section, we generalize the static version of DSelect- k , $\tilde{q}(\alpha, Z)$, to the per-example gating setting. The key idea is to make the gate’s parameters α and Z functions of the input, so that the gate can make decisions on a per-example basis. Note that many functional forms are possible for these parameters. For simplicity and based on our experiments, we choose to make α and Z linear functions of the input example. More formally, let $G \in \mathbb{R}^{k \times p}$, $W^{(i)} \in \mathbb{R}^{m \times p}$, $i \in [k]$, be a set of learnable parameters. Given an input example $x \in \mathbb{R}^p$, we set $\alpha = Gx$ and $z^{(i)} = W^{(i)}x$ in $\tilde{q}(\alpha, Z)$ (to simplify the presentation, we do not include bias terms). Thus, the per-example version

of DSelect-k is a function v defined as follows:

$$v(G, W, x) = \sum_{i=1}^k \sigma(Gx)_i r(S(W^{(i)}x)).$$

In the above, the term $r(S(W^{(i)}x))$ represents the i -th single expert selector, whose output depends on the example x ; thus different examples are free to select different experts. The term $\sigma(Gx)_i$ determines the input-dependent weight assigned to the i -th selector. The gate $v(G, W, x)$ is continuously differentiable in the parameters G and W , so we propose optimizing it using first-order methods. Similar to the case of static gating, if $S(W^{(i)}x)$ is binary for all $i \in [k]$, then each $r(S(W^{(i)}x))$ will select exactly one expert, and the example x will be assigned to at most k experts.

To encourage $S(W^{(i)}x)$, $i \in [k]$ to become binary, we introduce an entropy regularizer (similar in essence to that in static gating). However, unlike static gating, the regularizer here should be on a per-example basis, so that each example respects the cardinality constraint. By Proposition 2, for any $i \in [k]$, $r(S(W^{(i)}x))$ belongs to the probability simplex. Thus, for each example x in the training data, we introduce a regularization term of the form: $\Omega(W, x) := \sum_{i \in [k]} h(r(S(W^{(i)}x)))$, and minimize the following objective function:

$$\sum_{(x,y) \in \mathcal{D}} \left(\frac{1}{N} \ell \left(y, \sum_{i=1}^n f_i(x) v(G, W, x)_i \right) + \lambda \Omega(W, x) \right),$$

where λ is a non-negative hyperparameter. Similar to the case of static gating, we tune over a range of λ values, and we only consider the choices of λ that force the average number of selected experts per example to be less than or equal to k . If the application requires that the cardinality constraint be satisfied strictly for every example (not only on average), then annealing γ in the smooth-step function towards zero enforces this.

4 Experiments

We study the performance of the DSelect-k gate in the context of MTL and compare with state-of-the-art gates and baselines. In the rest of this section, we present experiments on the following real MTL datasets: MovieLens, Multi-MNIST, and Multi-Fashion MNIST. Moreover, in Appendix C, we present two additional experiments: (i) an experiment on data from a large-scale, real-world recommender system and (ii) an experiment on synthetic data (with up to 128 tasks), in which we study the predictive and expert selection performance and perform ablation studies.

Competing Methods: We focus on a multi-gate MoE, and study the DSelect-k and Top-k gates in the both static and per-example gating settings. In addition, we consider two MTL baselines. The first baseline is a MoE with a softmax gate (which uses all the available experts). The second is a *shared bottom* model [4], where all tasks share the same bottom layers, which are in turn connected to task-specific neural networks.

Experimental Setup: All competing models were implemented in TensorFlow 2. We used Adam [18] and Adagrad [7] for optimization, and we tuned the key hyperparameters using random grid search (with an average of 5 trials per grid point). Full details on the setup are in Appendix D.

4.1 MovieLens

Dataset: MovieLens [10] is a movie recommendation dataset containing records for 4,000 movies and 6,000 users. Following Wang et al. [37], for every user-movie pair, we constructed two tasks. Task 1 is a binary classification task for predicting whether the user will watch a particular movie. Task 2 is a regression task to predict the user’s rating (in $\{1, 2, \dots, 5\}$) for a given movie. We use 1.6 million examples for training and 200,000 for each of the validation and testing sets.

Experimental Details: We use the cross-entropy and squared error losses for tasks 1 and 2, respectively. We optimize a weighted average of the two losses, i.e., the final loss function is $\alpha(\text{Loss of Task 1}) + (1 - \alpha)(\text{Loss of Task 2})$, and we report the results for $\alpha \in \{0.1, 0.5, 0.9\}$. The same loss function is also used for tuning and testing. The architecture consists of a multi-gate

MoE with 8 experts, where each of the experts and the task-specific networks is composed of ReLU-activated dense layers. For each α , we tune over the optimization and gate-specific hyperparameters, including the number of experts to select (i.e., k in DSelect- k and Top- k). After tuning, we train each model for 100 repetitions (using random initialization) and report the averaged results. For full details, see Appendix D.1.

Results: In Table 1, we report the test loss and the average number of selected experts⁴. The results indicate that for all values of α , either one of our DSelect- k gates (static or per-example) outperforms the competing methods, in terms of both the test loss and the number of selected experts. In only one case ($\alpha = 0.1$), Top- k (static) performed marginally better than DSelect- k gate (static), but DSelect- k (per-example) achieves the best performance across all methods in this case. Notably, the softmax MoE is uniformly outperformed by the DSelect- k and Top- k gates, so sparsity in gating seems to be beneficial on this dataset. Moreover, there does not seem to be a clear winner between static and per-example gating: each performs better for certain α 's.

4.2 Multi-MNIST and Multi-Fashion MNIST

Datasets: We consider two image classification datasets: Multi-MNIST and Multi-Fashion [32], which are multi-task variants of the MNIST [20] and Fashion MNIST [38] datasets. We construct the Multi-MNIST dataset similar to Sabour et al. [32]: (i) we start by uniformly sampling two images from the MNIST dataset and overlaying them on top of each other, and (ii) we shift the first and second digits by 4 pixels (in each direction) towards the top-left and bottom-right corners, respectively. This procedure leads to 36×36 images with some overlap between the digits. The Multi-Fashion is constructed in a similar way by overlaying images from the Fashion MNIST dataset. For each dataset, we consider two classification tasks: Task 1 is to classify the top-left item and Task 2 is to classify the bottom-right item. We use 100,000 examples for training, and 20,000 examples for each of the validation and testing sets.

Experimental Details: We use cross-entropy loss for each of the tasks and optimize the sum of the two losses⁵. The model is a multi-gate MoE with 8 experts, where each expert is a convolutional neural network and each task-specific network is composed of a number of dense layers. We tune the optimization and gate-specific hyperparameters, including the number of experts to select (i.e., k in DSelect- k and Top- k), and use the average of the task accuracies as the tuning metric. After tuning, we train each model for 100 repetitions (using random initialization) and report the averaged results. For full details, see Appendix D.2.

Results: In Table 2, we report the test accuracy and the number of selected experts for the Multi-MNIST and Multi-Fashion MNIST datasets. On Multi-MNIST, DSelect- k (static) outperforms Top- k , in terms of both the task accuracies and number of selected experts. For example, it achieves over 1% improvement in Task 2's accuracy compared to Top- k (static). DSelect- k (static) comes close to the performance of the Softmax MoE, but uses less experts (1.7 versus 8 experts). Here the DSelect- k (per-example) does not offer improvement over the static variant (unlike the MovieLens dataset). On Multi-Fashion, we again see that the DSelect- k (static) performs best in terms of accuracy.

Table 1: Test loss (with standard error) and average number of selected experts on MovieLens. The parameter α determines the weight of Task 1's loss (see text for details). The test loss is multiplied by 10^4 .

		$\alpha = 0.1$		$\alpha = 0.5$		$\alpha = 0.9$	
		Loss	Experts	Loss	Experts	Loss	Experts
Static	DSelect- k	4015 ± 5	2.7	3804 ± 3	1.5	3690 ± 2	1.3
	Top- k	4012 ± 4	2.0	3818 ± 2	2.0	3693 ± 6	2.0
Per-example	DSelect- k	4006 ± 6	1.5	3823 ± 3	1.2	3679 ± 2	1.1
	Top- k	4027 ± 8	2.0	3841 ± 4	2.0	3741 ± 3	2.0
Baselines	Softmax MoE	4090 ± 1	8.0	3960 ± 3	8.0	3847 ± 10	8.0
	Shared Bottom	4037 ± 2	-	3868 ± 2	-	3687 ± 1	-

⁴The number of experts is averaged over tasks and training repetitions, so it may take non-integer values.

⁵Due to the symmetry in the problem, assigning the two tasks equal weights is a reasonable choice.

Table 2: Test accuracy (with standard error) and number of selected experts on Multi-MNIST/Fashion.

		Multi-MNIST			Multi-Fashion MNIST		
		Accuracy 1	Accuracy 2	Experts	Accuracy 1	Accuracy 2	Experts
Static	DSelect-k	92.56 \pm 0.03	90.98 \pm 0.04	1.7	83.78 \pm 0.05	83.34 \pm 0.05	1.8
	Top-k	91.93 \pm 0.06	90.03 \pm 0.08	4	83.44 \pm 0.07	82.66 \pm 0.08	4
Per-example	DSelect-k	92.42 \pm 0.03	90.7 \pm 0.03	1.5	83.69 \pm 0.04	83.13 \pm 0.04	1.5
	Top-k	92.27 \pm 0.03	90.45 \pm 0.03	4	83.66 \pm 0.04	83.15 \pm 0.04	4
Baselines	Softmax MoE	92.61 \pm 0.03	91.0 \pm 0.03	8	83.48 \pm 0.04	82.81 \pm 0.04	8
	Shared Bottom	91.3 \pm 0.04	89.47 \pm 0.04	-	82.05 \pm 0.05	81.37 \pm 0.06	-

5 Conclusion

We introduced DSelect-k: a continuously differentiable and sparse gate for MoE, which can be trained using first-order methods. Given a user-specified parameter k , the gate selects at most k of the n experts. Such direct control over the sparsity level is typically handled in the literature by adding a cardinality constraint to the optimization problem. One of the key ideas we introduced is a binary encoding scheme that allows for selecting k experts, without requiring any constraints in the optimization problem. We studied the performance of DSelect-k in MTL settings, on both synthetic and real datasets. Our experiments indicate that DSelect-k can achieve significant improvements in prediction and expert selection, compared to state-of-the-art MoE gates and MTL baselines.

Acknowledgements: Part of this work has been done when Hussein Hazimeh was at Google Research. At MIT, Hussein Hazimeh and Rahul Mazumder acknowledge research funding from the Office of Naval Research [Grant ONR-N000141812298].

References

- [1] Emmanuel Bengio, Pierre-Luc Bacon, Joelle Pineau, and Doina Precup. Conditional computation in neural networks for faster models. *CoRR*, abs/1511.06297, 2015. URL <http://arxiv.org/abs/1511.06297>.
- [2] Yoshua Bengio, Nicholas Léonard, and Aaron Courville. Estimating or propagating gradients through stochastic neurons for conditional computation. *arXiv preprint arXiv:1308.3432*, 2013.
- [3] Mathieu Blondel, Andre Martins, and Vlad Niculae. Learning classifiers with fenchel-young losses: Generalized entropies, margins, and algorithms. In *The 22nd International Conference on Artificial Intelligence and Statistics*, pages 606–615. PMLR, 2019.
- [4] Rich Caruana. Multitask learning. *Machine learning*, 28(1):41–75, 1997.
- [5] Jianbo Chen, Le Song, Martin Wainwright, and Michael Jordan. Learning to explain: An information-theoretic perspective on model interpretation. In *International Conference on Machine Learning*, pages 883–892. PMLR, 2018.
- [6] Gonalo M Correia, Vlad Niculae, and Andr  FT Martins. Adaptively sparse transformers. In *Proceedings of the 2019 Conference on Empirical Methods in Natural Language Processing and the 9th International Joint Conference on Natural Language Processing (EMNLP-IJCNLP)*, pages 2174–2184, 2019.
- [7] John Duchi, Elad Hazan, and Yoram Singer. Adaptive subgradient methods for online learning and stochastic optimization. *Journal of machine learning research*, 12(7), 2011.
- [8] David S Ebert, F Kenton Musgrave, Darwyn Peachey, Ken Perlin, and Steven Worley. *Texturing & modeling: a procedural approach*. Morgan Kaufmann, 2003.
- [9] William Fedus, Barret Zoph, and Noam Shazeer. Switch transformers: Scaling to trillion parameter models with simple and efficient sparsity. *arXiv preprint arXiv:2101.03961*, 2021.
- [10] F Maxwell Harper and Joseph A Konstan. The movielens datasets: History and context. *Acm transactions on interactive intelligent systems (tiis)*, 5(4):1–19, 2015.
- [11] Hussein Hazimeh, Natalia Ponomareva, Petros Mol, Zhenyu Tan, and Rahul Mazumder. The tree ensemble layer: Differentiability meets conditional computation. In Hal Daum  III and Aarti Singh, editors, *Proceedings of the 37th International Conference on Machine Learning*, volume 119 of *Proceedings of Machine Learning Research*, pages 4138–4148, Virtual, 13–18 Jul 2020. PMLR.
- [12] Yani Ioannou, Duncan Robertson, Darko Zikic, Peter Kotschieder, Jamie Shotton, Matthew Brown, and Antonio Criminisi. Decision forests, convolutional networks and the models in-between. *arXiv preprint arXiv:1603.01250*, 2016.
- [13] Robert A Jacobs. Bias/variance analyses of mixtures-of-experts architectures. *Neural computation*, 9(2):369–383, 1997.
- [14] Robert A Jacobs, Michael I Jordan, Steven J Nowlan, and Geoffrey E Hinton. Adaptive mixtures of local experts. *Neural computation*, 3(1):79–87, 1991.
- [15] Eric Jang, Shixiang Gu, and Ben Poole. Categorical reparameterization with gumbel-softmax. *arXiv preprint arXiv:1611.01144*, 2016.
- [16] Wenxin Jiang and Martin A Tanner. On the identifiability of mixtures-of-experts. *Neural Networks*, 12(9):1253–1258, 1999.
- [17] Michael I Jordan and Robert A Jacobs. Hierarchical mixtures of experts and the em algorithm. *Neural computation*, 6(2):181–214, 1994.
- [18] Diederik P. Kingma and Jimmy Ba. Adam: A method for stochastic optimization. In Yoshua Bengio and Yann LeCun, editors, *3rd International Conference on Learning Representations, ICLR 2015, San Diego, CA, USA, May 7-9, 2015, Conference Track Proceedings*, 2015.

- [19] Diederik P Kingma and Max Welling. Auto-encoding variational bayes. *arXiv preprint arXiv:1312.6114*, 2013.
- [20] Yann LeCun, Corinna Cortes, and CJ Burges. Mnist handwritten digit database. *ATT Labs [Online]*. Available: <http://yann.lecun.com/exdb/mnist>, 2, 2010.
- [21] Dmitry Lepikhin, HyoukJoong Lee, Yuanzhong Xu, Dehao Chen, Orhan Firat, Yanping Huang, Maxim Krikun, Noam Shazeer, and Zhifeng Chen. Gshard: Scaling giant models with conditional computation and automatic sharding. *arXiv preprint arXiv:2006.16668*, 2020.
- [22] Jiaqi Ma, Zhe Zhao, Xinyang Yi, Jilin Chen, Lichan Hong, and Ed H Chi. Modeling task relationships in multi-task learning with multi-gate mixture-of-experts. In *Proceedings of the 24th ACM SIGKDD International Conference on Knowledge Discovery & Data Mining*, pages 1930–1939, 2018.
- [23] Chris J Maddison, Andriy Mnih, and Yee Whye Teh. The concrete distribution: A continuous relaxation of discrete random variables. *arXiv preprint arXiv:1611.00712*, 2016.
- [24] Andre Martins and Ramon Astudillo. From softmax to sparsemax: A sparse model of attention and multi-label classification. In *International Conference on Machine Learning*, pages 1614–1623. PMLR, 2016.
- [25] Krzysztof Maziarczyk, Efi Kokipoulou, Andrea Gesmundo, Luciano Sbaiz, Gabor Bartok, and Jesse Berent. Gumbel-matrix routing for flexible multi-task learning. *arXiv preprint arXiv:1910.04915*, 2019.
- [26] Max Paulus, Dami Choi, Daniel Tarlow, Andreas Krause, and Chris J Maddison. Gradient estimation with stochastic softmax tricks. In H. Larochelle, M. Ranzato, R. Hadsell, M. F. Balcan, and H. Lin, editors, *Advances in Neural Information Processing Systems*, volume 33, pages 5691–5704. Curran Associates, Inc., 2020. URL <https://proceedings.neurips.cc/paper/2020/file/3df80af53dce8435cf9ad6c3e7a403fd-Paper.pdf>.
- [27] Ben Peters, Vlad Niculae, and André FT Martins. Sparse sequence-to-sequence models. In *Proceedings of the 57th Annual Meeting of the Association for Computational Linguistics*, pages 1504–1519, 2019.
- [28] Prajit Ramachandran and Quoc V Le. Diversity and depth in per-example routing models. In *International Conference on Learning Representations*, 2018.
- [29] Clemens Rosenbaum, Tim Klinger, and Matthew Riemer. Routing networks: Adaptive selection of non-linear functions for multi-task learning. In *International Conference on Learning Representations*, 2018.
- [30] Randi J Rost, Bill Licea-Kane, Dan Ginsburg, John Kessenich, Barthold Lichtenbelt, Hugh Malan, and Mike Weiblen. *OpenGL shading language*. Pearson Education, 2009.
- [31] Sebastian Ruder. An overview of multi-task learning in deep neural networks. *arXiv preprint arXiv:1706.05098*, 2017.
- [32] Sara Sabour, Nicholas Frosst, and Geoffrey E Hinton. Dynamic routing between capsules. In *Advances in neural information processing systems*, pages 3856–3866, 2017.
- [33] Noam Shazeer, Azalia Mirhoseini, Krzysztof Maziarczyk, Andy Davis, Quoc V. Le, Geoffrey E. Hinton, and Jeff Dean. Outrageously large neural networks: The sparsely-gated mixture-of-experts layer. In *5th International Conference on Learning Representations, ICLR 2017, Toulon, France, April 24-26, 2017, Conference Track Proceedings*, 2017.
- [34] Ximeng Sun, Rameswar Panda, Rogerio Feris, and Kate Saenko. Adashare: Learning what to share for efficient deep multi-task learning. In H. Larochelle, M. Ranzato, R. Hadsell, M. F. Balcan, and H. Lin, editors, *Advances in Neural Information Processing Systems*, volume 33, pages 8728–8740. Curran Associates, Inc., 2020. URL <https://proceedings.neurips.cc/paper/2020/file/634841a6831464b64c072c8510c7f35c-Paper.pdf>.

- [35] Hongyan Tang, Junning Liu, Ming Zhao, and Xudong Gong. Progressive layered extraction (ple): A novel multi-task learning (mtl) model for personalized recommendations. In *Fourteenth ACM Conference on Recommender Systems*, pages 269–278, 2020.
- [36] Xin Wang, Fisher Yu, Zi-Yi Dou, Trevor Darrell, and Joseph E Gonzalez. Skipnet: Learning dynamic routing in convolutional networks. In *Proceedings of the European Conference on Computer Vision (ECCV)*, pages 409–424, 2018.
- [37] Yuyan Wang, Zhe Zhao, Bo Dai, Christopher Fifty, Dong Lin, Lichan Hong, and Ed H Chi. Small towers make big differences. *arXiv preprint arXiv:2008.05808*, 2020.
- [38] Han Xiao, Kashif Rasul, and Roland Vollgraf. Fashion-mnist: a novel image dataset for benchmarking machine learning algorithms. *arXiv preprint arXiv:1708.07747*, 2017.
- [39] Sang Michael Xie and Stefano Ermon. Reparameterizable subset sampling via continuous relaxations. In *International Joint Conference on Artificial Intelligence*, 2019.
- [40] Zhe Zhao, Lichan Hong, Li Wei, Jilin Chen, Aniruddh Nath, Shawn Andrews, Aditee Kumthekar, Maheswaran Sathiamoorthy, Xinyang Yi, and Ed Chi. Recommending what video to watch next: a multitask ranking system. In *Proceedings of the 13th ACM Conference on Recommender Systems*, pages 43–51, 2019.

A Related Work

Stochastic Subset Selection: Here we provide additional discussion on the problem of sampling a k -subset from a discrete distribution. Paulus et al. [26] introduced Stochastic Softmax Tricks (SST), a generalization of the Gumbel-softmax trick that allows for efficient learning over combinatorial distributions in neural networks. On a high-level, this is achieved by (approximately) reparameterizing the sampling distribution as a random convex program that is amenable to differentiation. One application of SST is (stochastic) k -subset selection. Several related works also adapt the Gumbel-softmax trick for (stochastic) k -subset selection [5, 39].

While the approaches above share some similarity with our proposal, there are fundamental differences. First, as discussed in the main paper, our proposal aims at deterministic subset selection, whereas these approaches model the subsets as samples from a distribution and aim at learning the parameters of the distribution. Deterministic subset selection approaches (such as ours) are generally not competing with the sampling approaches: the appropriate approach depends on the application. In fact, the latter two approaches can be complementary, e.g., deterministic subset selection methods (relaxations of the Top- k operation) are used in Chen et al. [5], Xie and Ermon [39] as a building block for (stochastic) k -subset selection. In the synthetic experiment of Section C, we also compare against similar relaxations of the Top- k . Moreover, in applications that require sampling, the Gumbel softmax trick or its generalizations [26] can be applied on top of our proposed reformulation (by modeling the binary variables in our proposal as random variables), which will lead to a smaller sample space. Second, there is an important difference in what is being reparameterized: in our proposal we present a novel reparameterization of the cardinality-constrained optimization problem (using binary encoding), whereas the approaches above reparameterize the sampling distribution. Finally, we note that a direct application of the stochastic approaches to MoE leads to several issues beyond interpretability, which may need further research. For example, the choice of the noise distribution in the latter approaches will be critical and may require tuning over many candidate distributions to achieve good empirical performance—see Paulus et al. [26] for discussion on this issue. Moreover, the latter stochastic approaches require dense training unlike our proposed method, which can exploit sparsity for more efficient training.

MTL: In MTL, deep learning-based architectures that perform soft-parameter sharing, i.e., share model parameters partially, are proving to be effective at exploiting both the commonalities and differences among tasks [31]. One flexible architecture for soft-parameter sharing is the multi-gate MoE [22]. We use the multi-gate MoE in our experiments and compare both sparse and dense gates—Ma et al. [22] considered only dense gates. In addition, several works have recently considered gate-like structures for flexible parameter sharing in MTL. For instance, Sun et al. [34], Maziarz et al. [25] give each task the flexibility to use or ignore components inside the neural network. The decisions are modeled using binary random variables, and the corresponding probability distributions

are learned using SGD and the Gumbel-softmax trick [15]. This approach is similar to static gating, but it does not support per-example gating. Moreover, the number of nonzeros cannot be directly controlled (in contrast to our gate). Our work is also related to Rosenbaum et al. [29] who introduced “routers” (similar to gates) that can choose which layers or components of layers to activate per-task. The routers in the latter work are not differentiable and require reinforcement learning algorithms.

B Methodology Details

B.1 Proofs

Proof Proposition 1. Let $f = \{f_i\}_{i \in [n]}$. To prove equivalence, we need to establish the following two directions: (I) an optimal solution (f^*, α^*, Z^*) to Problem (5) can be used to construct a feasible solution (f, w) to Problem (2) and both solutions have the same objective, and (II) an optimal solution (f^*, w^*) to Problem (2) can be used to construct a feasible solution (f, α, Z) to Problem (5) and both solutions have the same objective. Direction (I) is trivial: the solution defined by $f = f^*$ and $w = q(\alpha^*, Z^*)$ is feasible for Problem (2) and has the same objective as (f^*, α^*, Z^*) .

Next, we show Direction (II). Let $s^* = \|w^*\|_0$ and denote by t_j the index of the j -th largest element in w^* , i.e., the nonzero entries in w^* are $w_{t_1}^* > w_{t_2}^* > \dots > w_{t_{s^*}}^*$. For every $i \in [s^*]$, set $z^{(i)}$ to the binary representation of $t_i - 1$. If $s^* < k$, then we set the remaining (unset) $z^{(i)}$ ’s as follows: for $i \in \{s^* + 1, s^* + 2, \dots, k\}$ set $z^{(i)}$ to the binary representation of $t_{s^*} - 1$. By this construction, the nonzero indices selected by $r(z^{(i)})$, $i \in [k]$ are exactly the nonzero indices of w^* .

To construct α , there are two cases to consider: (i) $s^* = k$ and (ii) $s^* < k$. If $s^* = k$, then set $\alpha_i = \log(w_{t_i}^*)$ for $i \in [k]$. Therefore, $\sigma(\alpha)_i = w_{t_i}^*$ for $i \in [k]$, and consequently $q(\alpha, Z) = w^*$. Otherwise, if $s^* < k$, then set $\alpha_i = \log(w_{t_i}^*)$ for $i \in [s^* - 1]$ and $\alpha_i = \log(w_{t_{s^*}}^* / (k - s^*))$ for $i \in [s^*, s^* + 1, \dots, k]$. Thus, for $i \in [s^* - 1]$, we have $\sigma(\alpha)_i = w_{t_i}^*$, i.e., the weights of the nonzero indices t_j , $j \in [s^* - 1]$ in $q(\alpha, Z)$ are equal to those in w^* . The weight assigned to the nonzero index t_{s^*} in $q(\alpha, Z)$ is: $\sum_{i \in [s^*, s^* + 1, \dots, k]} \sigma(\alpha)_i = \sum_{i \in [s^*, s^* + 1, \dots, k]} w_{t_{s^*}}^* / (k - s^*) = w_{t_{s^*}}^*$. Therefore, $q(\alpha, Z) = w^*$. In both (i) and (ii), we have $q(\alpha, Z) = w^*$, so the solution (f^*, α, Z) is feasible and has the same objective as (f^*, w^*) .

Proof of Proposition 2. First, we will use induction to show that $r(S(z))$ belongs to the probability simplex. Specifically, we will prove that for any integer $t \geq 1$ and $z \in \mathbb{R}^t$, $r(S(z))$ belongs to the probability simplex.

Our base case is for $t = 1$. In this case, there is a single binary encoding variable $z_1 \in \mathbb{R}$ and 2 experts. The single expert selector $r(S(z_1))$ is defined as follows: $r(S(z_1))_1 = 1 - S(z_1)$ and $r(S(z_1))_2 = S(z_1)$. The latter two terms are non-negative and sum up to 1. Thus, $r(S(z_1))$ belongs to the probability simplex.

Our induction hypothesis is that for some $t \geq 1$ and any $z \in \mathbb{R}^t$, $r(S(z))$ belongs to the probability simplex. For the inductive step, we need to show that for any $v \in \mathbb{R}^{t+1}$, $r(S(v))$ belongs to the probability simplex. From the definition of $r(\cdot)$, the following holds:

$$r(S(v))_i = \begin{cases} r(S([v_1, v_2, \dots, v_t]^T))_i (1 - S(v_{t+1})) & i \in [2^t] \\ r(S([v_1, v_2, \dots, v_t]^T))_{i-2^t} S(v_{t+1}) & i \in [2^{t+1}] \setminus [2^t] \end{cases} \quad (\text{B.8})$$

By the induction hypothesis, we have $r(S([v_1, v_2, \dots, v_t]^T))_i \geq 0$ for any i . Moreover, $S(\cdot)$ is a non-negative function. Therefore, $r(S(v))_i \geq 0$ for any i . It remains to show that the sum of the entries in $r(S(v))$ is 1, which we establish next:

$$\begin{aligned} \sum_{i=1}^{2^{t+1}} r(S(v))_i &= \sum_{i=1}^{2^t} r(S(v))_i + \sum_{i=2^t+1}^{2^{t+1}} r(S(v))_i \\ &\stackrel{(\text{B.8})}{=} \sum_{i=1}^{2^t} r(S([v_1, v_2, \dots, v_t]^T))_i (1 - S(v_{t+1})) + \sum_{i=2^t+1}^{2^{t+1}} r(S([v_1, v_2, \dots, v_t]^T))_{i-2^t} S(v_{t+1}) \end{aligned} \quad (\text{B.9})$$

Using a change of variable, the second summation in the above can be rewritten as follows: $\sum_{i=2^t+1}^{2^{t+1}} r(S([v_1, v_2, \dots, v_t]^T))_{i-2^t} S(v_{t+1}) = \sum_{i=1}^{2^t} r(S([v_1, v_2, \dots, v_t]^T))_i S(v_{t+1})$. Plugging the latter equality into (B.9) and simplifying, we get $\sum_{i=1}^{2^{t+1}} r(S(v))_i = 1$. Therefore, $r(S(v))$ belongs to the probability simplex, which establishes the inductive step. Finally, we note that $\tilde{q}(\alpha, Z)$ belongs to the probability simplex since it is a convex combination of probability vectors.

B.2 Extending DSelect-k to arbitrary n

Suppose that the number of experts n is not a power of 2. For the DSelect-k gate $\tilde{q}(\alpha, Z)$ to work in this setting, we need each single expert selector r used by the gate to be able to handle n experts. Next, we discuss how r can handle n when it is not a power of 2. Let m be the smallest integer so that $n < 2^m$. Then, we treat the problem as if there are 2^m experts and use a binary encoding vector $z \in \mathbb{R}^m$. For $i \in [n]$, we let entry $r(z)_i$ be the weight of expert i in the MoE. Note that the entries $r(z)_i, i \in \{n+1, n+2, \dots, 2^m\}$, are not associated with any experts. To avoid a situation where $r(z)$ assigns nonzero probability to the latter entries, we add the following penalty to the objective function: $\frac{\xi}{\sum_{i \in [n]} r(z)_i}$ where ξ is a non-negative parameter used to control the strength of the penalty. This penalty encourages $r(z)_i, i \in [n]$ (i.e., the entries associated with the n experts) to get more probability. In our experiments, we observe that $\sum_{i \in [n]} r(z)_i$ converges to 1, when ξ is sufficiently large. The penalty described above is part of our TensorFlow implementation of DSelect-k. We also note that there are other potential alternatives to deal with the entries $r(z)_i, i \in \{n+1, n+2, \dots, 2^m\}$, without adding a penalty to the objective function. For example, one alternative is to randomly assign each of $r(z)_i, i \in \{n+1, n+2, \dots, 2^m\}$ to one of the n experts.

B.3 Smooth-step Function

In Figure B.2, we plot the smooth-step function and the logistic function $L(x) = (1 + e^{-6x})^{-1}$. Note that the logistic function is re-scaled to be on the same scale as the smooth-step function.

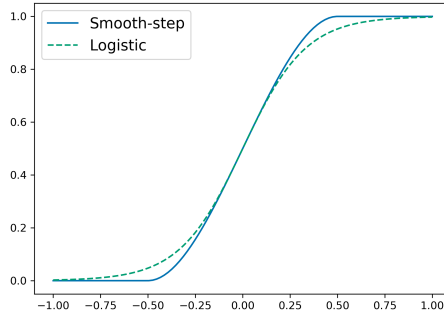


Figure B.2: The Smooth-step ($\gamma = 1$) and Logistic functions.

C Additional Experimental Results

C.1 A Real-world Large-scale Recommender System

We study the performance of DSelect-k and Top-k in a large-scale content recommendation system, deployed by Google. The recommendation system encompasses hundreds of millions of unique items and billions of users.

Recommender System Architecture and Dataset: The system consists of a candidate generator followed by a multi-task ranking model, and it adopts a framework similar to [40, 35]. The ranking model makes predictions for 6 classification and 2 regression tasks. These can be classified into two categories: (i) engagement tasks (e.g., predicting user clicks, bad clicks, engagement time), and (ii) satisfaction tasks (e.g., predicting user satisfaction behaviors such as likes and dislikes). We construct

the dataset from the system’s user logs (which contain historical information about the user and labels for the 8 tasks). The dataset consists of billions of examples⁶. We use a random 90/10 split for the training and evaluation sets.

Experimental Details: We use the cross-entropy and squared error losses for the classification and regression tasks, respectively. The ranking model is based on a multi-gate MoE, in which each task uses a separate static gate. The MoE uses 8 experts, where each is composed of dense layers. For each of the DSelect-k and Top-k based models, we tune the learning rate and the experts’ architecture. Then, using the best hyperparameters, we train the final models for 5 repetitions (using random initialization). For additional details, see Appendix D.3.

Table C.3: Performance metrics (AUC and RMSE) on a real-world recommendation dataset. The standard error is shown next to each value. Best values are in bold.

Tasks / Methods	DSelect-k	Top-k
Engagement Task 1 (AUC)	0.8103 \pm 0.0002	0.7481 \pm 0.0198
Engagement Task 2 (AUC)	0.8161 \pm 0.0002	0.7624 \pm 0.0169
Engagement Task 3 (RMSE)	0.2874 \pm 0.0002	0.3406 \pm 0.0180
Engagement Task 4 (RMSE)	0.8781 \pm 0.0014	1.1213 \pm 0.0842
Engagement Task 5 (AUC)	0.7524 \pm 0.0003	0.5966 \pm 0.0529
Satisfaction Task 1 (AUC)	0.6133 \pm 0.0066	0.5080 \pm 0.0047
Satisfaction Task 2 (AUC)	0.8468 \pm 0.0289	0.5981 \pm 0.0616
Satisfaction Task 3 (AUC)	0.9259 \pm 0.0008	0.6665 \pm 0.0091

Results: In Table C.3, we report the out-of-sample performance metrics for the 8 tasks. The results indicate that DSelect-k outperforms Top-k on all tasks, with the improvements being most pronounced on the satisfaction tasks. In Figure C.3, we show a heatmap of the expert weights chosen by the DSelect-k gates. Notably, for DSelect-k, all engagement tasks share at least one expert, and two of the satisfaction tasks share the same expert.

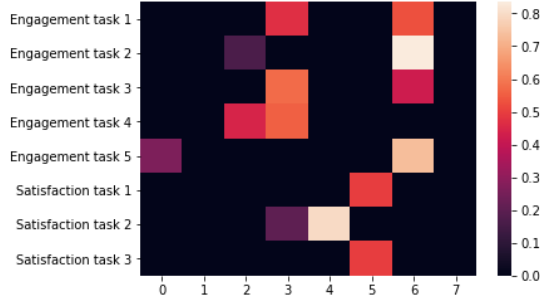


Figure C.3: Expert weights of the DSelect-k gates on the recommender system.

C.2 Prediction and Expert Selection Performance on Synthetic Data

In this experiment, we aim to (i) understand how the number of experts and tasks affects the prediction and expert selection performance for the different gates, and (ii) quantify the benefit from binary encoding in our gate through an ablation study. We focus on a static gating setting, where we consider the DSelect-k and Top-k gates, in addition to two variants of the DSelect-k gate used for ablation. To better quantify the expert selection performance and avoid model mis-specification, we use synthetic data generated from a multi-gate MoE. First, we describe our data generation process.

Synthetic Data Generation: We consider 128 regression tasks, separated into four mutually exclusive groups: $\{G_i\}_{i \in [4]}$, where G_i is the set of indices of the tasks in group i . As we will discuss next, the tasks are constructed in a way so that tasks within each group are highly related, while tasks across groups are only marginally related. Such a construction mimics real-world applications in which tasks can be clustered in terms of relatedness.

Each group consists of 16 tasks which are generated from a group-specific MoE. The group-specific MoE consists of 4 experts: $\{f_i\}_{i \in [4]}$. Each expert is the sum of 4 ReLU-activated units. The output

⁶We do not report the exact number for confidentiality.

of each task in the group is a convex combination of the 4 experts. Specifically, for each task $t \in [16]$ in the group, let $\alpha^{(t)} \in \mathbb{R}^4$ be a task-specific weight vector. Then, given an input vector x , the output of task t is defined as follows:

$$y^{(t)}(x) := \sum_{i=1}^4 \sigma(\alpha^{(t)})_i f_i(x)$$

For each group, we create an instance of the group-specific MoE described above, where we initialize all the weights randomly and independently from the other groups. In particular, we sample the weights of each expert independently from a standard normal distribution. To encourage relatedness among tasks in each group, we sample the task weights $[\alpha^{(1)}, \alpha^{(2)} \dots \alpha^{(16)}]$ from a zero-mean multivariate normal distribution where we set the correlation between any two task weights to 0.8.

To generate the data, we sample a data matrix X , with 140,000 observations and 10 features, from a standard normal distribution. The data matrix is shared by all 128 tasks and the regression outputs are obtained by using X as an input to each group-specific MoE. We use 100,000 observations for the training set and 20,000 observations for each of the validation and testing sets.

Experiment Design: We consider a multi-gate MoE and compare the following static gates: DSelect-k gate, Top-k gate, and an “ablation” gate (which will be discussed later in this section). Our goal is to study how, for each gate, the number of tasks affects the prediction and expert selection performance. To this end, we consider 4 regression problems, each for a different subset of the 128 tasks; specifically, we consider predicting the tasks in (i) G_1 (16 tasks), (ii) $G_1 \cup G_2$ (32 tasks), (iii) $G_1 \cup G_2 \cup G_3$ (64 tasks), and (iv) $G_1 \cup G_2 \cup G_3 \cup G_4$ (128 tasks). In each of the four problems, we use a multi-gate MoE to predict the outputs of the corresponding tasks simultaneously. The MoE has the same number of experts used to generate the data, i.e., if T is the total number of tasks in the problem, the MoE consists of $T/4$ experts, where the experts are similar to those used in data generation (but are trainable). Each task is associated with a task-specific gate, which chooses a convex combination of 4 out of the $T/4$ experts. Note that unlike the architecture used to generate the data, each task gate here is connected to all experts, even those belonging to the unrelated groups. The architecture used to generate the data can be recovered if the task gates across groups do not share experts, and the task gates within each group share the same 4 experts. We use squared error loss for training and tuning.

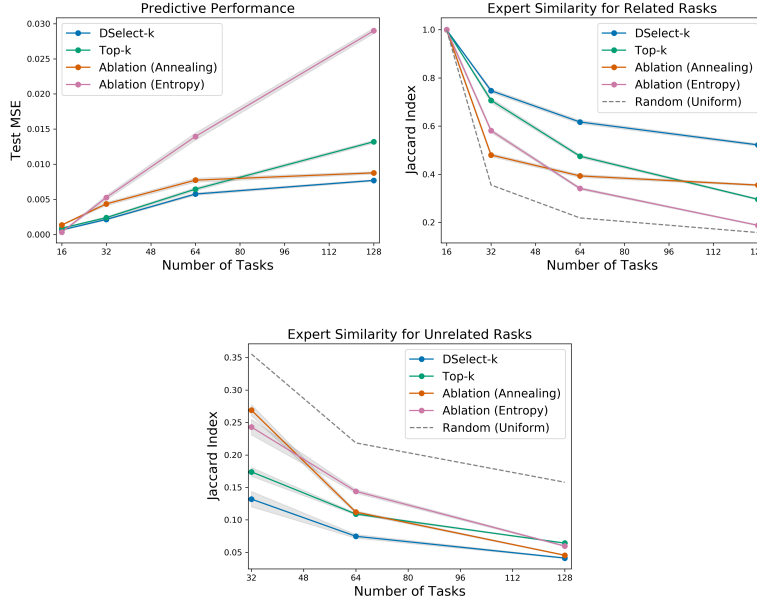


Figure C.4: Predictive and expert selection performance on synthetic data generated from a MoE.

Ablation: In addition to comparing the DSelect-k and Top-k gates, we perform an ablation study to gain insight on the role of binary encoding in the DSelect-k gate. Recall that in the DSelect-k

gate, we introduced the single expert selector which learns a one-hot encoded vector (using a binary encoding scheme). In the literature, a popular way to learn such one-hot encoded vectors is by using a softmax (with additional heuristics such as temperature annealing to ensure that the probability concentrates on one entry). Thus, in our ablation study, we consider the DSelect-k gate $\hat{q}(\alpha, Z)$, and we replace each single expert selector $r(\cdot)$ with a softmax-based selector. More precisely, let $\alpha \in \mathbb{R}^k$ and $\beta^{(i)} \in \mathbb{R}^n$, $i \in [k]$, be learnable parameter vectors. Then, we consider the following “ablation” gate: $h(\alpha, \beta) := \sum_{i=1}^k \sigma(\alpha)_i \sigma(\beta^{(i)})$. Here, $\sigma(\alpha)_i$ determines the weight assigned to selector i , and $\sigma(\beta^{(i)})$ acts as a surrogate to the single expert selector $r(S(z^{(i)}))$. To ensure that $\sigma(\beta^{(i)})$ selects a single expert (i.e., leads to a one-hot encoding), we consider two alternatives: (i) annealing the temperature of $\sigma(\beta^{(i)})$ during training⁷, and (ii) augmenting the objective with an entropy regularization term (similar to that of the DSelect-k gate) to minimize the entropy of each $\sigma(\beta^{(i)})$. In our results, we refer to (i) by “Ablation (Annealing)” and to (ii) by “Ablation (Entropy)”. Note that these two ablation alternatives can converge to a one-hot encoding asymptotically (due to the nature of the softmax), whereas our proposed gate can converge in a finite number of steps.

Measuring Expert Selection Performance: To quantify the similarity between the experts selected by the different tasks, we use the Jaccard index. Given two tasks, let A and B be the sets of experts selected by the first and second tasks, respectively. The Jaccard index of these two sets is defined by: $|A \cap B| / |A \cup B|$. In our experiments, we compute: (i) the average Jaccard index for the related tasks, and (ii) the average Jaccard index for unrelated tasks. Specifically, we obtain (i) by computing the Jaccard index for each pair of related tasks, and then averaging. We obtain (ii) by computing the Jaccard index over all pairs of tasks that belong to different groups (i.e., pairs in the same group are ignored), and then averaging.

Results: After tuning, we train each competing model, with the best hyperparameters, for 100 randomly-initialized repetitions. In Figure C.4, we plot the performance measures (averaged over the repetitions) versus the number of tasks. In the left plot, we report the MSE on the test set. In the middle and right plots we report the (averaged) Jaccard index for the related and unrelated tasks, respectively. In the latter two plots, we also consider a random gate which chooses 4 experts uniformly at random, and plot the expected value of its Jaccard index. In Figure C.4 (middle), a larger index is better since the related tasks will be sharing more experts. In contrast, in Figure C.4 (right), a lower index is preferred since the unrelated tasks will be sharing less experts. For all methods, the Jaccard index in Figures C.4 (middle) and (right) decreases with the number of tasks. This is intuitive, since as the number of tasks increases, we use more experts, giving any two given gates more flexibility in choosing mutually exclusive subsets of experts.

Overall, the results indicate that DSelect-k gate significantly outperforms Top-k in all the considered performance measures, and the differences become more pronounced as the number of tasks increases. For example, at 128 tasks, DSelect-k achieves over 40% improvement in MSE and 76% improvement in Jaccard index for related tasks, compared to Top-k. The DSelect-k gate also outperforms the two ablation gates in which we replace the binary encoding by a Softmax-based selector. The latter improvement suggests that the proposed binary encoding scheme is relatively effective at selecting the right experts. We also investigated the poor performance of the Ablation (Entropy) gate, and it turns out that the Softmax-based single expert selectors, i.e., the $\sigma(\beta^{(i)})$ ’s, tend to select the same expert. Specifically, we set $k = 4$ in the ablation gate, but it ends up selecting ~ 2 experts in many of the training repetitions. In contrast, the DSelect-k and Top-k gates select 4 experts.

C.3 Gate Visualizations

C.3.1 MovieLens

In Figure C.5, we plot the expert weights during training on the MovieLens dataset, for the Top-k and DSelect-k gates (after tuning both models). The plots show that Top-k exhibits frequent “jumps”, where in a single training step an expert’s weight can abruptly change from a nonzero value to zero. These jumps keep occurring till the end of training (at around 10^5 training steps). In contrast, DSelect-k has smooth transitions during training. Additional details on the MovieLens dataset and the MoE architecture used can be found in Section 4.1 of the paper.

⁷There are pathological cases where annealing the temperature in softmax will converge to more than one nonzero entry. This can happen when multiple entries in the input to the softmax have exactly the same value.

C.3.2 Synthetic Data

Here we consider a binary classification dataset generated from a static MoE that consists of 4 experts. We train another MoE model which employs 16 experts: 4 of these experts are copies (i.e., have exactly same weights) of the 4 experts used in data generation, and the rest of the experts are randomly initialized. We freeze all the experts and train only over the gate parameters. In this simple setting, we expect the gate to be able to recover the 4 experts that were used to generate the data. We trained two MoE models: one based on Top-k and another based on DSelect-k. After tuning both models, Top-k recovered only 1 right expert (and made 3 mistakes), whereas our model recovered all 4 experts. In Figures C.6 and C.7, we plot the expert weights during training, for the Top-k and DSelect-k gates, respectively. The Top-k exhibits a sharp oscillatory behavior during training, whereas DSelect-k has smooth transitions.

Additional details on data generation and model: We consider a randomly initialized “data-generating” MoE with 4 experts (each is a ReLU-activated dense layer with 4 units). The output of the MoE is obtained by taking the average of the 4 experts and feeding that into a single logistic unit. We generate a multivariate normal data matrix X with 20,000 observations and 10 features (10,000 observations are allocated for each of the training and validation sets). To generate binary classification labels, we use X as an input to the data-generating MoE and apply a sign function to the corresponding output. For training and tuning, we consider a MoE architecture with 16 experts: 4 of these experts are copies of the experts used in data generation, and the rest of the experts are initialized randomly. All experts are frozen (not trainable). A trainable gate chooses 4 out of the 16 experts, and the final result is fed into a single logistic unit. We optimized the cross-entropy loss using Adam with a batch size of 256, and tuned over the learning rate $\{10^{-1}, 10^{-2}, \dots, 10^{-5}\}$.

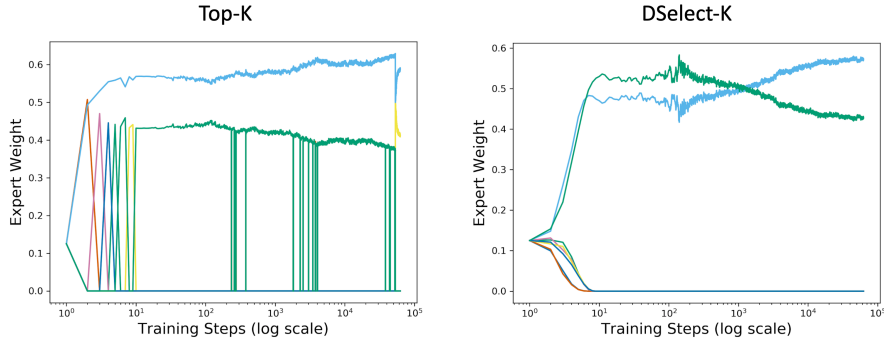


Figure C.5: Expert weights during training on the MovieLens dataset. Each color corresponds to a separate expert. The plots are for the best models obtained after tuning.

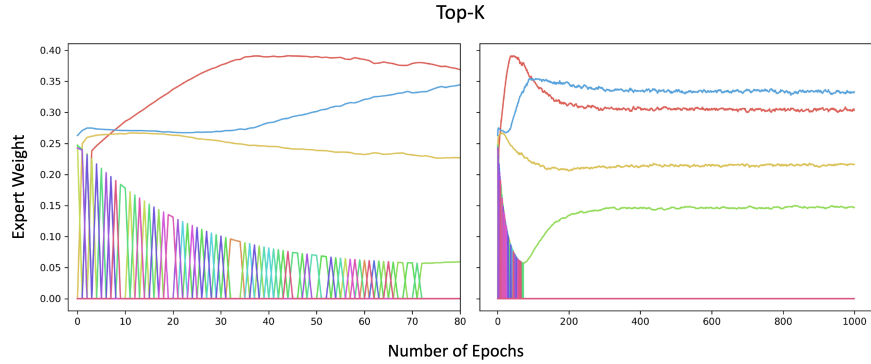


Figure C.6: Expert weights during training on synthetic data generated from a MoE. Each color corresponds to a separate expert. The left plot is a magnified version of the right plot. The plots are for the best model obtained after tuning.

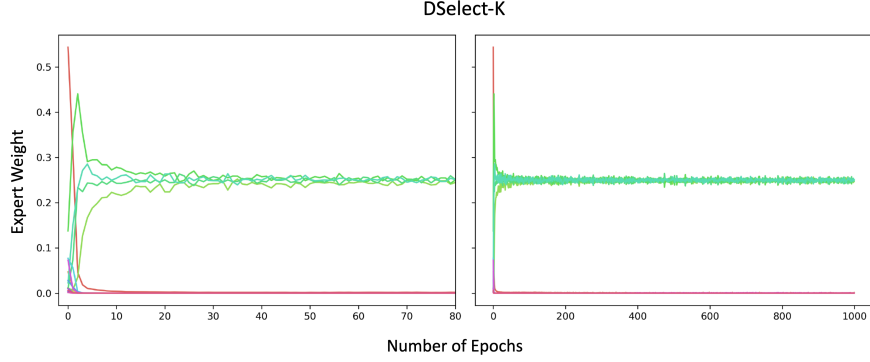


Figure C.7: Expert weights during training on synthetic data generated from a MoE. Each color corresponds to a separate expert. The left plot is a magnified version of the right plot. The plots are for the best model obtained after tuning.

C.4 Gate Convergence and FLOPS

In Table C.4, we report the percentage of training steps required for $S(Z)$ to converge to a binary matrix in the DSelect-k gate, on several real datasets. These results are based on the tuned models discussed in Section 4 of the paper. We also report the number of floating point operations (FLOPS) required by the MoE based on DSelect-k relative to the MoE based on Top-k, during training. The results indicate that the number of training steps till convergence to a binary matrix depends on the specific dataset: ranging from only 0.04% on the MovieLens dataset to 80% on the Multi-Fashion MNIST. Moreover, on certain datasets (MovieLens with $\alpha = 0.9$ and Multi-MNIST), DSelect-k requires less FLOPS during training than Top-k, i.e., DSelect-k is effective at conditional training (on these particular datasets).

Table C.4: We report two statistics: (i) Percentage of training steps required for the DSelect-k gate to converge to a binary matrix, and (ii) the number of FLOPS needed by the DSelect-k based MoE during training relative to that of Top-k. The parameter α controls the weight assigned to task 1’s loss in the MovieLens dataset—see Section 4.1 of the paper for more details.

	MovieLens			Multi-MNIST	Multi-Fashion
	$\alpha = 0.1$	$\alpha = 0.5$	$\alpha = 0.9$		
% Training Steps until Binary $S(Z)$	11.37	9.39	0.04	42.33	80.02
FLOPS(DSelect-k)/FLOPS(Top-k)	1.5	1.2	0.6	0.8	1.2

D Experimental Details

Computing Setup: We ran the experiments on a cluster that automatically allocates the computing resources. For confidentiality, we do not report the exact specifications of the cluster.

D.1 MovieLens

Architecture: For MoE-based models, we consider a multi-gate MoE architecture (see Figure 1), where each task is associated with a separate gate. The MoE uses 8 experts, each of which is a ReLU-activated dense layer with 256 units, followed by a dropout layer (with a dropout rate of 0.5). For each of the two tasks, the corresponding convex combination of the experts is fed into a task-specific subnetwork. The subnetwork is composed of a dense layer (ReLU-activated with 256 units) followed by a single unit that generates the final output of the task. The shared bottom model uses a dense layer (whose number of units is a hyperparameter) that is shared by the two tasks, followed by a dropout layer (with a rate of 0.5). For each task, the output of the shared layer is fed into a task-specific subnetwork (same as that of the MoE-based models).

Hyperparameters and Tuning: We tuned each model using random grid search, with an average of 5 trials per grid point. We used Adagrad with a batch size of 128 and considered the following hyperparameters and ranges: Learning Rate: $\{0.001, 0.01, 0.1, 0.2, 0.3\}$, Epochs: $\{5, 10, 20, 30, 40, 50\}$, k for Top- k and DSelect- k : $\{2, 4\}$, λ for DSelect- k : $\{0.1, 1, 10\}$, γ for smooth-step: $\{1, 10\}$, Units in Shared bottom: $\{32, 256, 2048, 4096, 8192\}$.

D.2 Multi-MNIST and Multi-Fashion MNIST

Architecture: MoE-based models use a multi-gate MoE (as in Figure 1). Each of the 8 experts is a CNN that is composed (in order) of: (i) convolutional layer 1 (kernel size = 5, number of filters = 10, ReLU-activated) followed by max pooling, (ii) convolutional layer 2 (kernel size = 5, number of filters = 20, ReLU-activated) followed by max pooling, and (iii) a stack of ReLU-activated dense layers with 50 units each (the number of layers is a hyperparameter). The subnetwork specific to each task is composed of a stack of 3 dense layers: the first two have 50 ReLU-activated units and the third has 10 units followed by a softmax. The shared bottom model uses a shared CNN (with the same architecture as the CNN in the MoE). For each task, the output of the shared CNN is fed into a task-specific subnetwork (same as that of the MoE-based models).

Hyperparameters and Tuning: We tuned each model using random grid search, with an average of 5 trials per grid point. We used Adam with a batch size of 256 and considered the following hyperparameters and ranges: Learning Rate: $\{0.01, 0.001, 0.0001, 0.00001\}$, Epochs: $\{25, 50, 75, 100\}$, k for Top- k and DSelect- k : $\{2, 4\}$, γ for smooth-step: $\{0.1, 1, 10\}$, Number of dense layers in CNN: $\{1, 3, 5\}$.

D.3 Recommender System

Each of the 8 experts in the MoE consists of a stack of ReLU-activated dense layers with 256 units each. We fix $K = 2$ in both DSelect- k and Top- k . We tune over the learning rate and architecture. For both models, training is terminated when there is no significant improvement in the validation loss.

D.4 Synthetic Data

We tuned each model using random grid search, with an average of 5 trials per grid point. We used Adam with a batch size of 256 and considered the following hyperparameters and ranges: Learning rate: $\{0.001, 0.01, 0.1\}$, Epochs $\{25, 50, 75, 100\}$, γ for smooth-step: $\{5, 10, 15\}$, λ for DSelect- k : $\{0.001, 0.005, 0.01, 0.1\}$, λ for Ablation (Entropy): $\{10^{-6}, 10^{-5}, 10^{-4}, 10^{-3}, 10^{-2}, 10^{-1}, 1, 100\}$. Moreover, for Ablation (Annealing), we anneal the temperature of softmax starting from a hyperparameter s down to 10^{-16} (the temperatures are evenly spaced on a logarithmic scale). We tune the starting temperature s over $\{10^{-6}, 10^{-5}, 5 \times 10^{-5}, 10^{-4}, 2.5 \times 10^{-4}, 5 \times 10^{-4}, 7.5 \times 10^{-4}, 10^{-3}, 5 \times 10^{-3}, 10^{-2}\}$ (note that such a fine grid was necessary to get annealing to work for the ablation gate).